Hindawi
International Journal of RF and Microwave Computer-Aided Engineering
Volume 2023, Article ID 9025980, 8 pages
https://doi.org/10.1155/2023/9025980

Research Article

A Miniaturized Low-Loss Switchable Single- and Dual-Band Bandpass Filter

Ruonan Mu,[1] **Yongle Wu**,[1] **Leidan Pan**,[1] **Wei Zhao**,[1] **and Weimin Wang**[2]

[1]*School of Integrated Circuits, Beijing University of Posts and Telecommunications, Beijing, China*
[2]*School of Electronic Engineering, Beijing University of Posts and Telecommunications, Beijing, China*

Correspondence should be addressed to Yongle Wu; ywu@bupt.edu.cn

Received 12 April 2023; Revised 10 July 2023; Accepted 5 August 2023; Published 18 August 2023

Academic Editor: Xiao Ding

In this paper, a novel switchable bandpass filter is proposed. By switching p-i-n diodes on/off, the proposed filter can be switched between the single-band bandpass filter and the dual-band bandpass filter. The filter is mainly composed of eight pairs of series LC resonators, which generate passbands and transmission zeros. Considering the requirement of miniaturization and low cost, the filter is realized by interdigital capacitors and microstrip section inductors. The layout is designed by 3D simulation software HFSS, and the active part is designed by ADS software. The proposed filter has a compact structure, and its size is only 22.20 mm × 25.66 mm. For a demonstration, a switchable bandpass filter has been designed, fabricated, and measured. The simulated and measured results have a good agreement.

1. Introduction

Microwave bandpass filter [1–5] has been widely used in wireless communication systems as a frequency selection device for the RF front-end. With the rapid development of wireless communication systems and the increasing demand for communication, RF devices should be designed to achieve more functions. Switchable filters have become the focus of researches in recent years, and various RF devices for designing switchable filters have been reported, such as RF p-i-n diodes [6], varactors [7], SPDT switches [8], and liquid metal actuation [9].

With the development of modern technology, there are many methods to design switchable filters. For example, a compact switchable filter based on parallel-coupled lines is presented in [10], which has three different filtering functions. In [11], a novel reconfigurable filter using transversal signal-interaction principles is proposed, which has three different switchable filtering states, such as the ultra-wideband bandpass filter, the narrow-band bandpass filter, and the ultra-wideband bandstop filter. In [12], a reconfigurable filter switching between a bandpass response and a bandstop response using the substrate-integrated evanescent-mode cavity resonators is designed. An independently switched, reconfigurable dual-band filter with high isolation between two adjacent frequency bands is proposed in [13], which reports the design method of the dual-band bandpass filter with the diode-loaded resonator. Bandpass-to-bandstop switchable filters using radio frequency micro-electromechanical system switch are presented [14], which are implemented in both single- and dual-band versions with variable fractional bandwidth. A switchable microstrip bandpass filter with reconfigurable on-state frequency responses [15] is proposed, which consists of a two-pole BPF and two switchable delay lines. Furthermore, a novel microstrip switchable bandpass filter is presented [16], which could provide three different filtering states, such as the broadband bandpass filter, the dual-band bandpass filter, and the tri-band bandpass filter by switching RF p-i-n diodes on/off. However, the sizes of the above microstrip filters are limited by the physical wavelength of the microstrip lines, making them have difficulty in achieving the miniaturization goal of the filter.

In this paper, a novel switchable bandpass filter using interdigital capacitors and microstrip section inductors is proposed. It has two different filter states, including the

bandpass filter (BPF) and the dual-band bandpass filter (DBPF), and the two filter states can be switched by controlling the on-off of the p-i-n diodes. The filter is composed of eight pairs of LC resonators, which produce four transmissions zeros and enhance the rejection ability of the stopband and the frequency selectivity. Furthermore, the transmission zeros can be controlled independently. All lumped elements in this filter are realized by interdigital capacitors and microstrip section inductors, which have the advantages of simple process, strong stability, and high integration. These filters are useful in many applications, such as wireless communication systems, military electronics, and radar systems.

2. Design Theory

Figure 1 shows the circuit schematic of the proposed switchable bandpass filter. This switchable filter has two different filtering states including the bandpass filter and the dual-band bandpass filter. Furthermore, two filtering states can be switched by switching the p-i-n diodes on/off. As shown in Figure 1, when switches 1 and 1' are turned OFF, the switchable filter becomes a BPF, while when switches 1 and 1' are turned ON, the proposed switchable filter becomes a DBPF.

2.1. Bandpass Filter (State I). Figure 2 shows the circuit schematic of the bandpass filter section in the proposed switchable filter, which contains five pairs of series LC resonators. C_1 and L_1 in the middle part form the passband of the bandpass filter, L_2 and C_2 generate a transmission zero (TZ) at the lower frequency of the passband, and L_3 and C_3 generate a transmission zero at the higher frequency of the passband, which improves the frequency selection performance of the filter. Z_0 is the terminal impedance and is set to 50 Ω. The ideal simulated results of the designed bandpass filter are shown in Figure 3. There are two transmission zeros (TZs), which are located at 2.07 and 3.31 GHz. Besides, there are two transmission poles (TPs), which are located at 2.63 and 2.76 GHz.

Since the structure of the circuit is symmetric, the circuit can be analyzed by the even- and odd-mode analysis methods [17]. The even-mode circuit is shown in Figure 4(a), and the odd-mode circuit is shown in Figure 4(b).

The equivalent impedance Z_{ine} of the even-mode circuit in Figure 4(a) can be calculated as follows:

$$Z_{ine} = \frac{1}{j\omega C_4} + \frac{Z_{ine1}(j\omega L_3 + (1/j\omega C_3))}{Z_{ine1} + (j\omega L_3 + (1/j\omega C_3))},$$
$$Z_{ine1} = \frac{1}{j\omega(C_1(C_2/2)/(C_1 + (C_2/2)))} + j\omega(L_1 + 2L_2). \quad (1)$$

The equivalent impedance Z_{ino} of the odd-mode circuit in Figure 4(b) can be calculated as follows:

$$Z_{ino} = 1/j\omega C_4 + \frac{(j\omega L_3 + (1/j\omega C_3))(j\omega L_1 + (1/j\omega C_1))}{(j\omega L_3 + (1/j\omega C_3)) + (j\omega L_1 + (1/j\omega C_1))}. \quad (2)$$

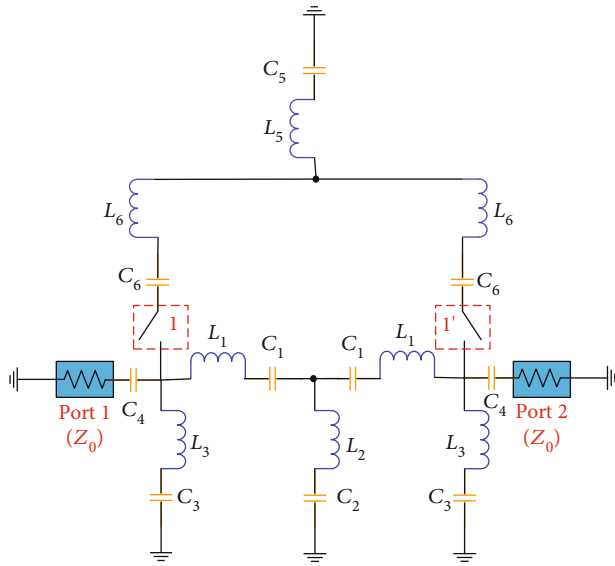

Figure 1: The circuit schematic of the proposed switchable filter.

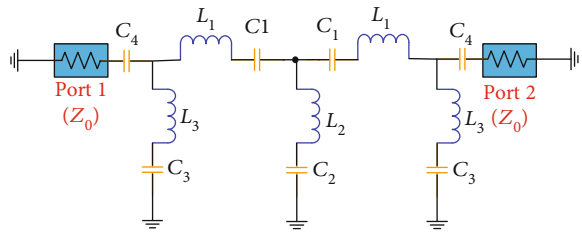

Figure 2: Lumped-element circuit schematic of the bandpass filter section in the proposed switchable filter.

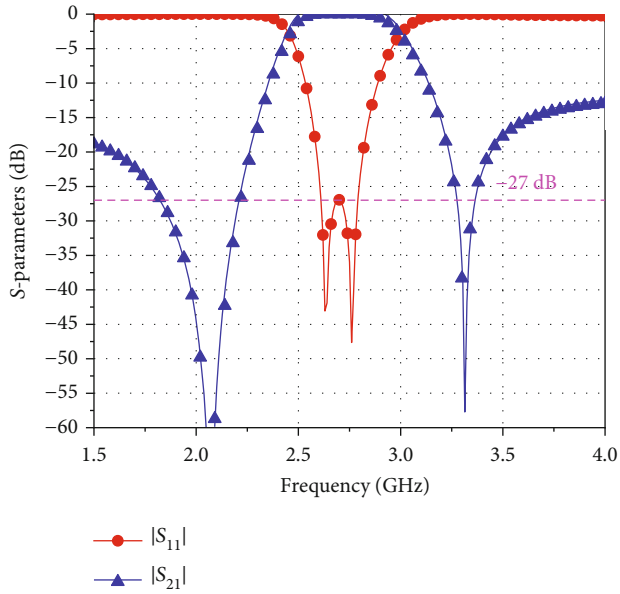

Figure 3: Ideal simulated S-parameters for the bandpass filter.

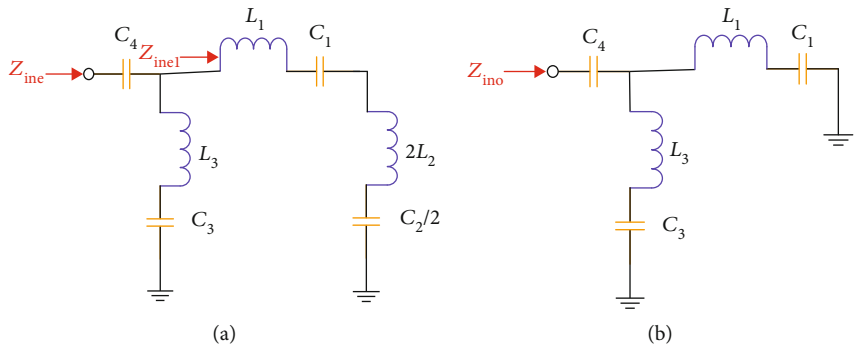

FIGURE 4: (a) The even-mode circuit and (b) the odd-mode circuit of the proposed bandpass filter.

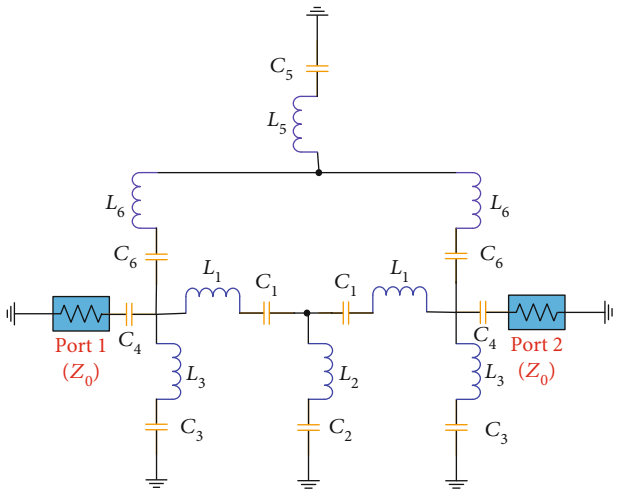

FIGURE 5: Lumped-element circuit schematic of the dual-band filter section in the proposed switchable filter.

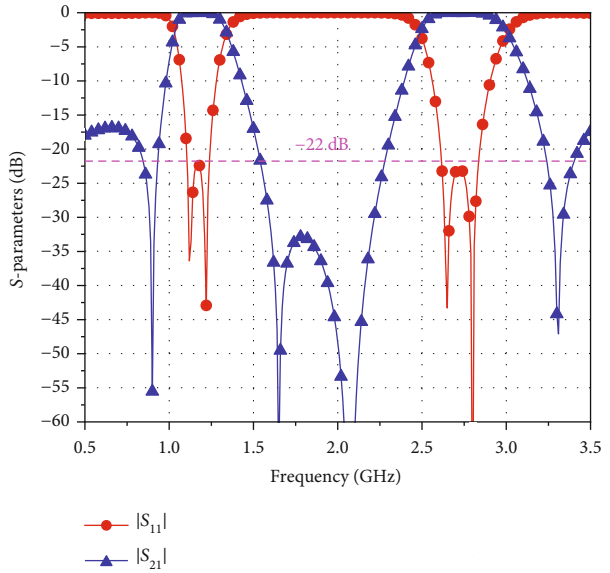

FIGURE 6: Ideal simulated S-parameters for the dual-band bandpass filter.

The transmission coefficient S_{21} can be calculated as follows [17]:

$$S_{21} = \frac{(Z_{ine}Z_0 - Z_{ino}Z_0)}{(Z_0 + Z_{ine})(Z_0 + Z_{ino})}. \quad (3)$$

By setting $S_{21} = 0$, two transmission zeros can be obtained as follows:

$$f_{Z1} = \frac{1}{2\pi\sqrt{L_3C_3}}, \quad (4)$$

$$f_{Z2} = \frac{1}{2\pi\sqrt{L_2C_2}}. \quad (5)$$

According to (4) and (5), f_{z1} is inversely proportional to L_3 and C_3, and similarly, f_{z2} is inversely proportional to L_2 and C_2. TZ_1 can be independently controlled by C_3 when the value of L_3 is fixed, and similarly, when the value of C_3 is fixed, TZ_1 can be independently controlled by L_3. Besides, C_2 and L_2 can control TZ_2 independently. Moreover, as L_2, C_2, L_3, and C_3 increase, both TZ_1 and TZ_2 move towards lower frequencies.

From the above analysis, it can be concluded that two transmission zeros of the bandpass filter (TZ_1 and TZ_2) can be independently controlled and do not affect each other [18].

2.2. Dual-Band Bandpass Filter (State II). Figure 5 shows the circuit schematic of the dual-band filter section in the proposed switchable filter. The circuit is composed of the above BPF and three series LC resonators in parallel. The first passband of this DBPF is controlled by L_5, C_5, L_6, and C_6, where L_5 and C_5 can control the bandwidth of the first passband; in addition, L_6 and C_6 can control the position of the first center frequency. The ideal simulated results of the designed dual-band bandpass filter are shown in Figure 6.

Since the structure of this dual-band filter is symmetric, the circuit can be analyzed by the even- and odd-mode analysis methods. The odd-mode circuit is shown in Figure 7(a), and the even-mode circuit is shown in Figure 7(b).

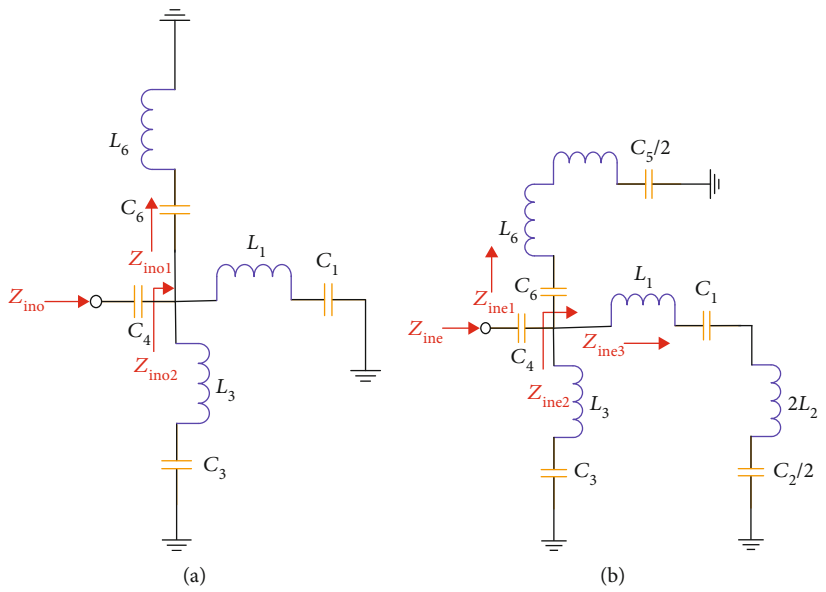

FIGURE 7: (a) The odd-mode circuit and (b) the even-mode circuit of the proposed dual-band bandpass filter.

The equivalent impedance Z_{ino} of the odd-mode circuit in Figure 7(a) can be calculated as follows:

$$
\begin{aligned}
Z_{ino} &= \frac{1}{j\omega C_4} + \frac{Z_{ino1}Z_{ino2}}{Z_{ino1}+Z_{ino2}},\\
Z_{ino1} &= \frac{1}{j\omega C_6} + j\omega L_6,\\
Z_{ino2} &= \frac{(j\omega L_3 + (1/j\omega C_3))(j\omega L_1 + (1/j\omega C_1))}{(j\omega L_3 + (1/j\omega C_3)) + (j\omega L_1 + (1/j\omega C_1))}.
\end{aligned}
\tag{6}
$$

The equivalent impedance Z_{ine} of the even-mode circuit in Figure 7(b) can be calculated as follows:

$$
\begin{aligned}
Z_{ine} &= \frac{1}{j\omega C_4} + \frac{Z_{ine1}Z_{ine2}}{Z_{ine1}+Z_{ine2}},\\
Z_{ine1} &= \frac{1}{j\omega((C_6(C_5/2))/(C_6+(C_5/2)))} + j\omega(L_6+2L_5),\\
Z_{ine2} &= \frac{Z_{ine3}(j\omega L_3 + (1/j\omega C_3))}{Z_{ine3}+(j\omega L_3+(1/j\omega C_3))},\\
Z_{ine3} &= \frac{1}{j\omega(C_1(C_2/2)/(C_1+(C_2/2)))} + j\omega(L_1+2L_2).
\end{aligned}
\tag{7}
$$

2.3. Switchable Bandpass Filter. The final complete circuit structure of the proposed switchable filter is shown in Figure 8. The bias circuits required for the p-i-n diodes are added, containing two inductors and the DC power supply V_{dc}. In addition, in order to eliminate the DC component, it is necessary to parallel a capacitor C_7 with a large capacitance value at both the input and output ports. The lumped element parameters of the switchable bandpass filter are listed in Table 1. The ideal simulated results of the two states in the proposed switchable bandpass filter are shown in Figure 9.

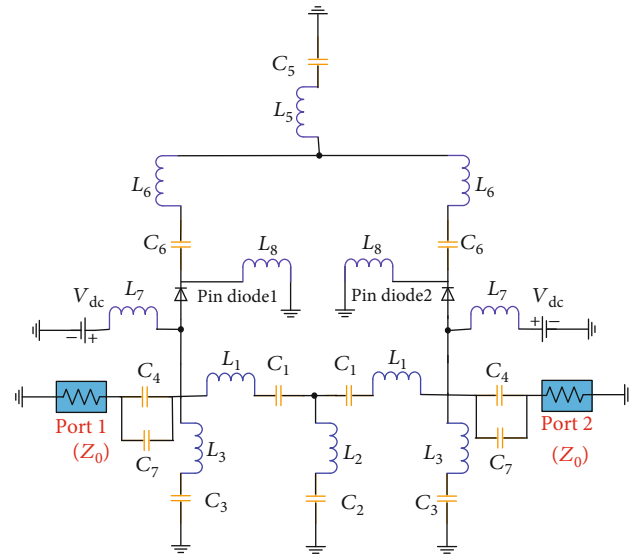

FIGURE 8: The full circuit schematic of the proposed switchable filter.

TABLE 1: Lumped element parameters of the switchable bandpass filter.

C_1	L_1	C_2	L_2	C_3	L_3	C_4
0.7 pF	4.1 nH	0.7 pF	3.3 nH	0.7 pF	5.9 nH	15 pF
C_5	L_5	C_6	L_6	C_7	L_7	L_8
2.7 pF	12.7 nH	1 pF	18.3 nH	680 pF	390 nH	390 nH

The filter designed is realized by interdigital capacitors and microstrip section inductors. The layout of the interdigital capacitor is shown in Figure 10(a). It has multiple

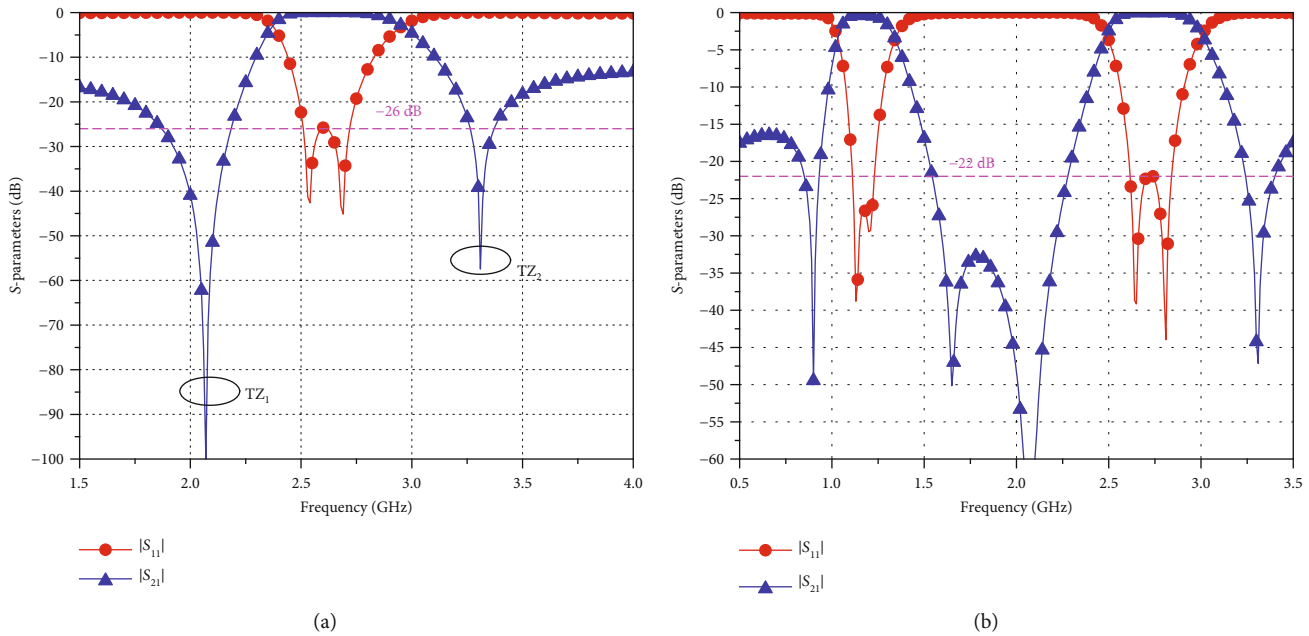

FIGURE 9: Ideal simulated S-parameters for the proposed switchable bandpass filter. (a) State I. (b) State II.

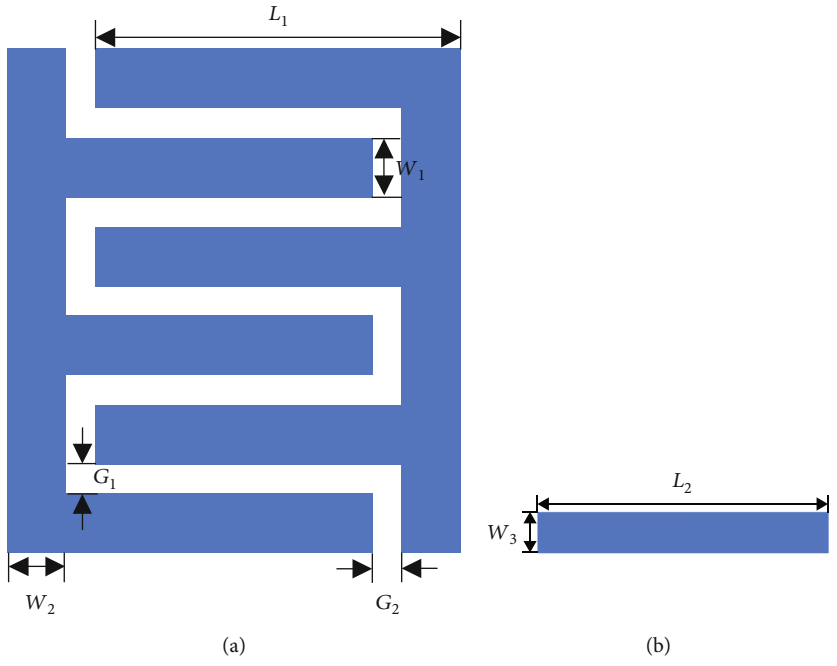

FIGURE 10: The layout of (a) interdigital capacitor and (b) microstrip inductor.

geometric variables, including L_1, W_1, W_2, G_1, G_2, and N (the number of fingers). The capacitance value is extracted by the following formula (Y_{12} is the admittance of the interdigital capacitor):

$$C = -\frac{\mathrm{Im}\,(Y_{12})}{2\pi f}. \tag{8}$$

Similarly, Figure 10(b) shows the layout of the microstrip inductor, and its inductance value is extracted by the following formula (Y_{11} is the admittance of the microstrip inductor):

$$L = -\frac{1}{2\pi f Im(Y_{11})}. \tag{9}$$

Therefore, by properly adjusting the structure of interdigital capacitors and the microstrip inductors (including L_1, W_1, W_2, G_1, G_2, N, L_2, and W_3), the interdigital capacitors and the microstrip inductors corresponding to the lumped

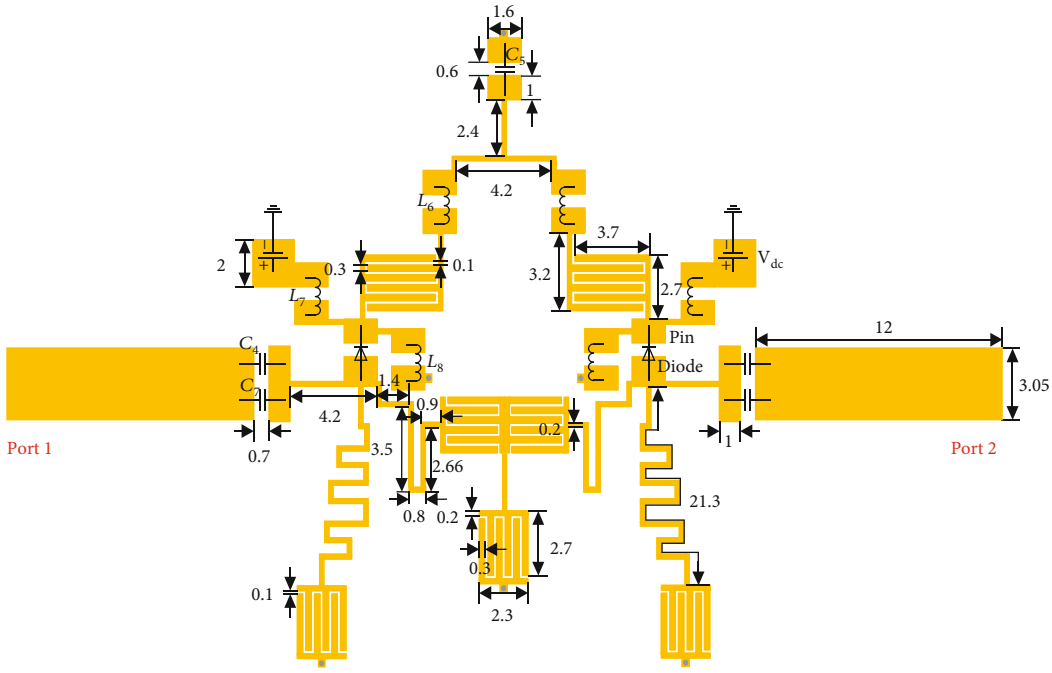

(a)

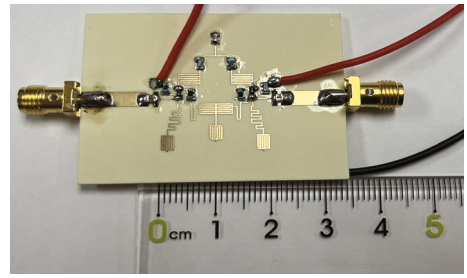

(b)

FIGURE 11: (a) Layout of the proposed switchable bandpass filter. (b) Practical photograph (unit: mm).

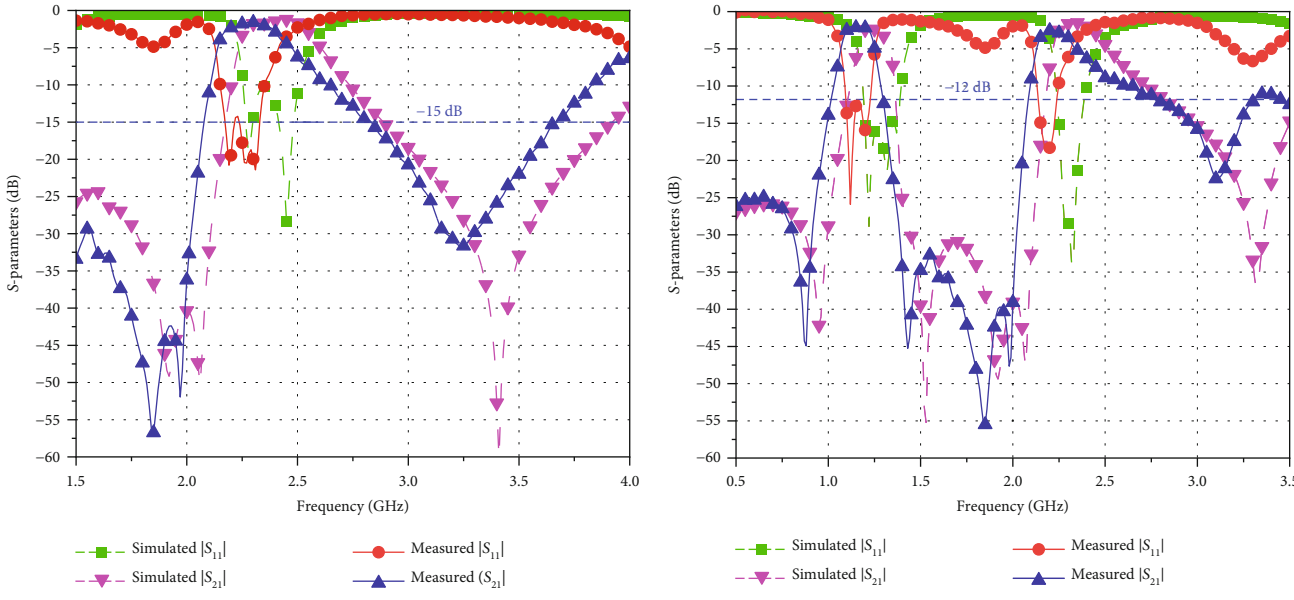

(a) (b)

FIGURE 12: EM simulated and measured the results of the proposed switchable filters. (a) State I. (b) State II.

Table 2: The performance comparison for the switchable filters.

Refs.	Responses	3-dB fractional bandwidth (%)	Return loss (dB)	Inband insertion loss (dB)	Number of diodes	Circuit size (mm^2)
[10]	BPF/BSP/DBPF	53.1/30.2/3.8 and 2.7	>12/-/>10	>0.9/>15.5/>2.2	6	42.23×27.84
[11]	$BPF_1/BPF_2/BSF$	95.7/25.3/106.0	>11.4/>15/-	>0.94/>0.8/>15.0	6	30.71×15.36
[13]	$BPF_1/BPF_2/DBPF$	11.0/10.5/11.4 and 10.8	>20*/>19*/>22*	>3.05/>3.1/>3.0	4	60.84×75.45
[15]	BPF_1/BPF_2	9.0/9.0	>10*/>12*	>3.0*/>2.0*	2	54.40×50.20
This work	BPF/DBPF	13.7/15.8 and 11.2	>14/<18.8	>1.6/>2.0	2	22.20×25.66

*: estimated value.

parameters in the circuit structure in Figure 1 can be obtained.

Based on the above analysis, the design procedure of the proposed switchable bandpass filter is as follows:

(1) Specify the desired parameters including the center frequencies and bandwidths of two states, respectively

(2) Determine the circuit structure of the bandpass filter. By adjusting the values of C_1 and L_1, the BPF can meet the required center frequency. According to the center frequency and bandwidth, determine the approximate positions of the transmission zeros and select the appropriate values of inductors and capacitors

(3) Design another structure, which can be connected in parallel with the above BPF to obtain the DBPF. Then, select the values of inductors and capacitors

(4) Use the electromagnetic simulation software HFSS to establish the layout of the DBPF. The inductors are realized by the microstrip section inductors, and the capacitors are realized by the interdigital capacitors

(5) Use HFSS to reasonably optimize the size of the overall structure to obtain better performance

(6) In HFSS, the positions of the p-i-n diodes and the bias circuits are replaced by the pads, and then the simulation results are imported into the ADS software

(7) In ADS, add the required p-i-n diodes and other devices to obtain the final simulation results

3. Simulated and Measured Results

For a demonstration, a switchable bandpass filter based on the printed circuit board (PCB) technology has been designed, fabricated, and measured. In this paper, Rogers RO4350 is used as the dielectric substrate of the filter. Its relative permittivity is 3.66, the loss tangent is 0.004, and the thickness of the substrate is 1.524 mm. RF p-i-n diodes SMP1331-079LF from Skyworks are used for electronic switches. The MuRata lumped components are used. The layout of the proposed switchable bandpass filter and the practical photograph are shown in Figure 11.

The Rohde & Schwarz ZVA67 vector network analyzer is used for testing, and Figure 12 shows the EM simulation and test results of the proposed filter. There are small deviations and slight frequency shifts between the simulated and measured frequency responses, which may be attributed to the parasitic effects, the fabrication errors, and the measurement errors [19, 20].

As shown in Figure 12, under the BPF state, the measured passband 3-dB FBW is 13.7% with the center frequency 2.3 GHz. The measured insertion loss is 1.59 dB at the center frequency. The return loss is greater than 14 dB in the passband. Under the DBPF state, the measured two passbands 3-dB FBWs are 15.8% and 11.2% with the center frequency 1.16 and 2.25 GHz, respectively. The measured insertion losses are 2.0 and 2.46 dB at two center frequencies. The return loss is greater than 12 dB in the first passband and lower than 18.8 dB in the second passband.

To highlight the advantages of the proposed switchable bandpass filter, Table 2 lists the results of the comparison between the switchable bandpass filter designed in this paper and the filters in the references. It shows that the switchable bandpass filter designed in this paper has attained low insertion loss, compact size, and high return loss. Meanwhile, different states can be realized with less p-i-n diodes.

4. Conclusion

In this paper, a novel switchable bandpass filter has been proposed and implemented based on the PCB technology. Based on even- and odd-mode circuits, the design theory of the filter is described in detail. Furthermore, the filter is realized by interdigital capacitors and microstrip section inductors. The simulated and measured results have a good agreement, which verifies that the proposed filter has the advantages of simple design, compact size, low loss, high selectivity, and easy integration in the application of wireless communication systems.

Data Availability

The data that support the findings of this study are available on request from the corresponding author. The data are not publicly available due to privacy or ethical restrictions.

Conflicts of Interest

The authors declare that they have no conflicts of interest.

Acknowledgments

This work was supported by the National Natural Science Foundations of China (no. U22A2014 and no. U20A20203) and the Fundamental Research Funds for the Central Universities (2021XD-A07-2).

References

[1] M. Á. Sánchez-Soriano and C. Quendo, "Systematic design of wideband bandpass filters based on short-circuited stubs and $\lambda/2$ transmission lines," *IEEE Microwave and Wireless Components Letters*, vol. 31, no. 7, pp. 849–852, 2021.

[2] X. Dai, Q. Yang, H. Du, C. Guo, and A. Zhang, "Direct synthesis method for dual-band bandpass filters with wide fractional bandwidth range and center frequency ratio," *IEEE Transactions on Circuits and Systems II: Express Briefs*, vol. 68, no. 8, pp. 2755–2759, 2021.

[3] M. Fan, K. Song, and Y. Fan, "Reconfigurable bandpass filter with wide-range bandwidth and frequency control," *IEEE Transactions on Circuits and Systems II: Express Briefs*, vol. 68, no. 6, pp. 1758–1762, 2021.

[4] J. Xu, W. Wu, and G. Wei, "Novel dual-band bandpass filter and reconfigurable filters using lumped-element dual-resonance resonators," *IEEE Transactions on Microwave Theory and Techniques*, vol. 64, no. 5, pp. 1496–1507, 2016.

[5] W. Zhao, Y. Wu, Y. Yang, and W. Wang, "LTCC bandpass filter chips with controllable transmission zeros and bandwidths using stepped-impedance stubs," *IEEE Transactions on Circuits and Systems II: Express Briefs*, vol. 69, no. 4, pp. 2071–2075, 2022.

[6] A. Miller and J. S. Hong, "Wideband bandpass filter with reconfigurable bandwidth," *IEEE Microwave and Wireless Components Letters*, vol. 20, no. 1, pp. 28–30, 2010.

[7] H.-J. Tsai, B.-C. Huang, N.-W. Chen, and S.-K. Jeng, "A reconfigurable bandpass filter based on a varactor-perturbed, T-shaped dual-mode resonator," *IEEE Microwave and Wireless Components Letters*, vol. 24, no. 5, pp. 297–299, 2014.

[8] T.-H. Lee, J.-J. Laurin, and K. Wu, "Reconfigurable filter for bandpass-to-absorptive bandstop responses," *IEEE Access*, vol. 8, pp. 6484–6495, 2020.

[9] S. N. Mcclung, S. Saeedi, and H. H. Sigmarsson, "Band-reconfigurable filter with liquid metal actuation," *IEEE Transactions on Microwave Theory and Techniques*, vol. 66, no. 6, pp. 3073–3080, 2018.

[10] D. Li and K.-D. Xu, "Multifunctional switchable filter using coupled-line structure," *IEEE Microwave and Wireless Components Letters*, vol. 31, no. 5, pp. 457–460, 2021.

[11] W. Feng, Y. Shang, W. Che, R. Gómez-García, and Q. Xue, "Multifunctional reconfigurable filter using transversal signal-interaction concepts," *IEEE Microwave and Wireless Components Letters*, vol. 27, no. 11, pp. 980–982, 2017.

[12] E. J. Naglich, J. Lee, D. Peroulis, and W. J. Chappell, "A tunable bandpass-to-bandstop reconfigurable filter with independent bandwidths and tunable response shape," *IEEE Transactions on Microwave Theory and Techniques*, vol. 58, no. 12, pp. 3770–3779, 2010.

[13] P.-H. Deng and J.-H. Jheng, "A switched reconfigurable high-isolation dual-band bandpass filter," *IEEE Microwave and Wireless Components Letters*, vol. 21, no. 2, pp. 71–73, 2011.

[14] N. Kumar and Y. K. Singh, "RF-MEMS-based bandpass-to-bandstop switchable single- and dual-band filters with variable FBW and reconfigurable selectivity," *IEEE Transactions on Microwave Theory and Techniques*, vol. 65, no. 10, pp. 3824–3837, 2017.

[15] W.-H. Tu, "Switchable microstrip bandpass filters with reconfigurable on-state frequency responses," *IEEE Microwave and Wireless Components Letters*, vol. 20, no. 5, pp. 259–261, 2010.

[16] Z. Sun, X. Wang, and K. Li, "A switchable bandpass filter for broadband, dual-band and tri-band operations," *IEEE Transactions on Circuits and Systems II: Express Briefs*, vol. 70, no. 1, pp. 111–115, 2023.

[17] R. Li, S. Sun, and L. Zhu, *Microwave Bandpass Filters for Wideband Communications*, Wiley, Hoboken, NJ, USA, 2012, chs. 2 and 3.

[18] Y. Wu, L. Hao, W. Wang, and Y. Yang, "Miniaturized and low insertion loss diplexer using novel inter-digital capacitors and microstrip section inductors," *IEEE Transactions on Circuits and Systems II: Express Briefs*, vol. 69, no. 11, pp. 4303–4307, 2022.

[19] Y. Wu, L. Cui, Z. Zhuang, W. Wang, and Y. Liu, "A simple planar dual-band bandpass filter with multiple transmission poles and zeros," *IEEE Transactions on Circuits and Systems II: Express Briefs*, vol. 65, no. 1, pp. 56–60, 2018.

[20] J. S. Hong and M. J. Lancaster, *Microstrip Filter for RF/Microwave Applications*, John Wiley & Sons, New York, NY, USA, 2004.